



# optica

## Entangled coherent states created by mixing squeezed vacuum and coherent light

YONATAN ISRAEL,<sup>1,2</sup> LIOR COHEN,<sup>3,4</sup> XIN-BING SONG,<sup>1</sup> JAEWOO JOO,<sup>5,6</sup> HAGAI S. EISENBERG,<sup>3</sup> AND YARON SILBERBERG<sup>1</sup>

<sup>1</sup>Department of Physics of Complex Systems, Weizmann Institute of Science, Rehovot 76100, Israel

<sup>2</sup>Physics Department, Stanford University, 382 Via Pueblo Mall, Stanford, California 94305, USA

<sup>3</sup>Racah Institute of Physics, Hebrew University of Jerusalem, Jerusalem 91904, Israel

<sup>4</sup>Hearne Institute for Theoretical Physics, and Department of Physics and Astronomy, Louisiana State University, Baton Rouge, Louisiana 70803, USA

<sup>5</sup>School of Electronic and Electrical Engineering, University of Leeds, Leeds, LS2 9JT, UK

<sup>6</sup>Clarendon Laboratory, University of Oxford, Parks Road, Oxford OX1 3PU, UK

\*Corresponding author: [yisrael@stanford.edu](mailto:yisrael@stanford.edu)

Received 2 January 2019; revised 28 April 2019; accepted 1 May 2019 (Doc. ID 356121); published 29 May 2019

Entangled coherent states are a fundamentally interesting class of quantum states of light, with important implications in quantum information processing, for which robust schemes to generate them are required. Here, we show that entangled coherent states emerge, with high fidelity, when mixing coherent and squeezed vacuum states of light on a beam splitter. These maximally entangled states, where photons bunch at the exit of a beam splitter, are measured experimentally by Fock-state projections. Entanglement is examined theoretically using a Bell-type nonlocality test and compared with ideal entangled coherent states. We experimentally show nearly perfect similarity with entangled coherent states for an optimal ratio of coherent and squeezed vacuum light. In our scheme, entangled coherent states are generated deterministically with small amplitudes, which could be beneficial, for example, in deterministic distribution of entanglement over long distances. © 2019 Optical Society of America under the terms of the [OSA Open Access Publishing Agreement](https://doi.org/10.1364/OPTICA.6.000753)

<https://doi.org/10.1364/OPTICA.6.000753>

### 1. INTRODUCTION

Entanglement is a defining feature of quantum mechanics with important implications to fundamental concepts, as well as for applications. Quantum states of light that exhibit entanglement were extensively employed in tests of the foundations of quantum theory [1–3] and are essential in quantum computing, quantum communication, and quantum metrology [4,5]. An intriguing class of states is the entangled coherent states (ECSs), which contain CSs  $|\alpha\rangle$  in an equal superposition of being in either one of two possible paths [6–8]:

$$|\psi_{\text{ECS}}^{\alpha}\rangle = \mathcal{N}_{\alpha}(|\alpha, 0\rangle + |0, \alpha\rangle), \quad (1)$$

where  $\mathcal{N}_{\alpha} = 1/\sqrt{2(1 + e^{-|\alpha|^2})}$  is a normalization factor.

ECSs manifest entanglement of CSs—the most classical physical states—and are therefore fundamentally intriguing as they describe CSs that are entangled with the vacuum [Eq. (1)]. These states are also potentially useful in various applications of quantum technology. It has been suggested that ECSs could be advantageous resources for quantum information processing and quantum metrology [8], showing high tolerance against lossy quantum channels and interferometers [9,10], as well as reaching the Heisenberg limit in interferometry.

To create ECS, it has been suggested to make use of other nonclassical Schrödinger cat-states known as (even) CS superpositions (CSSs) [8,11]:

$$|\psi_{\text{CSS}}^{\beta}\rangle = \tilde{\mathcal{N}}_{\beta}(|\beta\rangle + |-\beta\rangle), \quad (2)$$

where  $\tilde{\mathcal{N}}_{\beta} = 1/\sqrt{2(1 + e^{-2|\beta|^2})}$ . Experimental realizations of CSS [12,13] and then of ECS [14] have relied mainly on a non-deterministic technique involving photon subtraction, a probabilistic approach that is typically inefficient. Deterministic schemes for generating CSS and ECS could be significantly more resource effective. Such techniques using nonlinear interferometry were studied theoretically [15–17], but so far were not experimentally demonstrated [8,18]. In this work, we demonstrate experimentally a deterministic method for generating ECS by using deterministic squeezed vacuum (SV) and CS sources, and without resorting to probabilistic approaches in generating ECS, such as photon subtraction or post-selection [14].

ECSs share similar properties with another class of entangled states, known as NOON states,

$$|\psi_{\text{NOON}}^N\rangle = (|N, 0\rangle + |0, N\rangle)/\sqrt{2}, \quad (3)$$

where  $N$  photons, rather than CSs, are superposed in two modes. ECSs comprise superpositions of NOON states [7], and both are capable of measurement sensitivities at the Heisenberg limit. While realizing NOON states and ECSs with high intensities has been a long-standing challenge [8,19], since both states are prone to loss, ECSs were proven to be more resilient in the context of quantum metrology [10,20].

Recently, it has been shown that mixing of coherent and SV light could give rise to superpositions of NOON states [21,22], which were demonstrated up to  $N = 5$  [23–25]. In that approach, NOON states resulted from post-selecting  $N$  photons after interfering SV and CS on a beam splitter (BS), rather than producing individual NOON states of fixed  $N$ . In the current work, we show theoretically and experimentally that the same system can be used to generate deterministically low-amplitude ECSs with high fidelity.

## 2. THEORETICAL ANALYSIS

Figure 1(a) illustrates schematically a process for preparing a perfect ECS  $|\psi_{\text{ECS}}^\alpha\rangle$  by mixing a CS ( $|\beta\rangle$ ) with a CSS  $|\psi_{\text{CSS}}^\beta\rangle$  on a 50/50 BS. Here  $\beta = \alpha/\sqrt{2}$  [11], and the average photon number in this state is

$$\bar{n} = |\alpha|^2 / (1 + e^{-|\alpha|^2}). \quad (4)$$

### A. Squeezed Vacuum and Coherent State Interference

Consider now a similar system, where a CS  $|\beta\rangle_a$  is mixed with a SV state  $|\xi\rangle_b$  on a 50% BS, as shown in Fig. 1(b). These input states can be defined in Fock basis [26] as

$$|\beta\rangle = e^{-|\beta|^2/2} \sum_{n=0}^{\infty} \frac{\beta^n}{\sqrt{n!}} |n\rangle, \quad \beta = |\beta|e^{i\phi}, \quad (5)$$

$$|\xi\rangle = \frac{1}{\sqrt{\cosh r}} \sum_{m=0}^{\infty} (-1)^m \frac{\sqrt{(2m)!}}{2^m m!} (e^{i\theta} \tanh r)^m |2m\rangle, \quad (6)$$

where the phases of  $|\beta\rangle$  and  $|\xi\rangle$  are  $\phi$  and  $\theta$ , respectively, while the relative phase of the two input states is  $\theta - \phi$ . The state at the output of the BS in modes  $c$  and  $d$  [Fig. 1(b)] is denoted by  $|\psi_{\text{out}}\rangle$ . The probability of  $|\psi_{\text{out}}\rangle_{c,d}$  for  $N_c$  and  $N_d$  photons simultaneously at the output of the BS is given by [27]

$$P_{N_c, N_d}(\beta, r, \theta) = |\langle N_c, N_d | \psi_{\text{out}} \rangle_{c,d}|^2. \quad (7)$$

### B. Fidelity of ECS with Mixed CS and SV

Now, we show that the state  $|\psi_{\text{out}}\rangle_{c,d}$  that is obtained when we mix a CS not with the ideal CSS state, but rather with a SV state, is still a good approximation of the ECS. It should be noted that both SV [Eq. (6)] and CSS [Eq. (2)] are composed of only even photon numbers and can be made approximately similar [28].

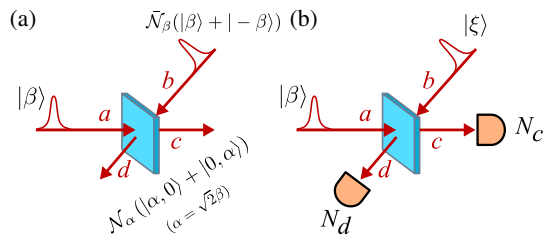


**Fig. 1.** Schematics for generating (a) ideal and (b) approximated entangled coherent states (ECSs). A 50/50 beam splitter combines a coherent state  $|\beta\rangle$  at port  $a$  and (a) coherent state superpositions (CSSs)  $\tilde{N}_\beta(|\beta\rangle + |-\beta\rangle)$  at port  $b$  to result with an exact ECS  $\mathcal{N}_\alpha(|\alpha, 0\rangle + |0, \alpha\rangle)$  in ports  $c, d$ . (b) When the squeezed vacuum state  $|\xi\rangle$  enters port  $b$  instead of CSS, the result in ports  $c, d$  approximates ECS (see text). In our experiment, a joint photon number measurement  $N_c, N_d$  is performed at modes  $c, d$ , respectively, using photon number-resolving detectors.

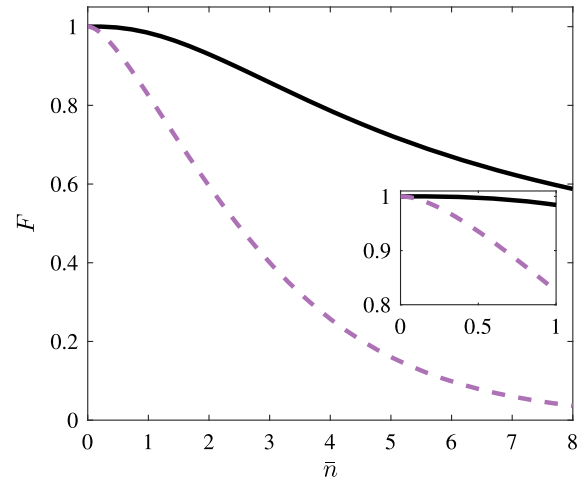


**Fig. 2.** Fidelity between ECS and states generated by mixing CS and SV,  $F = |\langle \psi_{\text{ECS}}^\alpha | \psi_{\text{out}} \rangle|^2$ , for the optimal SV amplitude as a function of the total photon number on average  $\bar{n}$  [Eq. (4)] in solid black. The inset shows  $F$  for low values of the average photon number. The fidelity between CSS and the vacuum state ( $|\text{vac}\rangle = |0\rangle$ ) is presented for comparison in dashed purple.

This similarity can be evaluated through the fidelity between the two states [29]:

$$\begin{aligned} F &= |\langle \psi_{\text{ECS}}^\alpha | \psi_{\text{out}} \rangle|^2 = \left| \langle \psi_{\text{CSS}}^{\alpha/\sqrt{2}} | \xi \rangle \right|^2 \\ &= \frac{1}{\cosh r \cosh\left(\frac{|\alpha|^2}{2}\right)} e^{-\frac{|\alpha|^2}{2}(\cos(\theta-2\phi) \tanh r)}. \end{aligned} \quad (8)$$

An optimal value of this fidelity [Eq. (8)] is achieved for the following parameter relation:

$$r = \text{arcsinh}(|\alpha|^2)/2, \quad \theta = 2\phi + \pi, \quad (9)$$

where Eq. (9) conditions the amplitude and phase of the SV to that of the CSS (see Supplement 1).

In Fig. 2, the solid line presents the fidelity [Eq. (8)] for the optimal values of SV [Eq. (9)], showing that indeed nearly perfect low amplitude ECS can be achieved using CS and SV, i.e.,  $F \approx 1$  for  $\bar{n}, |\alpha| < 1$ . However, for higher photon numbers, namely,  $\bar{n}, |\alpha| > 1$ , the resulting states are only an approximation of ECS, which deteriorates with increasing  $\bar{n}$ . We note that the criteria in Eq. (9) for the weak amplitudes regime ( $\alpha, r \ll 1$ ) coincides with the condition of setting the number of photon pairs of CS and SV to be equal, as needed for generating NOON states [21–23]. The fidelity between CSS and the vacuum state (Fig. 2, dashed line) is shown for comparison; this fidelity corresponds to the case of replacing the SV [Fig. 1(b)] with the vacuum state [Eq. (8)], while the CS remains the other input to the BS. Note that the fidelity in this classical case is lower than the fidelity between ECS and the states generated by mixing CS and SV for all average photon numbers (see Fig. 2). Although the size of the ECS amplitude is relatively small, it can still violate the Bell inequality, as will be shown next.

### C. Nonlocality and the Janssens Inequality

A unique quantum property of ECS relates to its nonlocal correlations, whereby multiple particles are all in one mode or the

other. Such nonlocal properties are typically examined through the violation of Bell inequalities [26]. ECSs were previously shown to violate several types of such Bell-type inequalities, including a modified version of the Janssens inequalities [30,31], which use measurements of phase-space operators [7]. We show here theoretically that the approximate ECSs that result from mixing a CS and SV violates the inequalities as well. Measuring these inequalities in experiment requires homodyne detection, and is not accessible with our current detection setup.

We recall the expectation values of single- and two-mode phase-space operators on modes  $c$  and  $d$ :

$$Q_c(\mu) = \langle \psi_{\text{out}} | \hat{Q}_c(\mu) \otimes \hat{I}_d | \psi_{\text{out}} \rangle, \quad (10)$$

$$Q_d(\nu) = \langle \psi_{\text{out}} | \hat{I}_c \otimes \hat{Q}_d(\nu) | \psi_{\text{out}} \rangle, \quad (11)$$

$$Q_{c,d}(\mu, \nu) = \langle \psi_{\text{out}} | \hat{Q}_c(\mu) \otimes \hat{Q}_d(\nu) | \psi_{\text{out}} \rangle. \quad (12)$$

Here,  $\hat{Q}_j(\mu) = |\mu\rangle\langle\mu|$  is a projection operator of the state in mode  $j$  onto a CS of complex amplitude  $\mu$ , and  $\hat{I}_j$  is the unity operator acting on mode  $j$  (for  $j = c, d$ ). Following Ref. [31], a modified version of the third Janssens inequality can then be written as

$$J_3 = Q(\alpha) - Q(\alpha, \beta) - Q(\alpha, \gamma) - Q(\alpha, \delta) + Q(\beta, \gamma) + Q(\beta, \delta) + Q(\gamma, \delta) \leq 0, \quad (13)$$

where  $\alpha, \beta, \gamma$ , and  $\delta$  are any complex number. In Eq. (13), the mode indices are omitted, meaning the  $Q(\alpha)$  can be measured in either mode  $c$  or  $d$ , and the joint two-mode expectation values are always measured between modes  $c$  and  $d$ .

A minimizing procedure carried out on the parameters  $\alpha, \beta, \gamma, \delta$  leads to a violation of the inequality  $J_3 \leq 0$ ; this is shown in Fig. 3 for any given average photon number of the states generated in our scheme,  $|\psi_{\text{out}}\rangle$ , as well as for ECS, following a  $\pi/2$  phase shift in mode  $d$  (Fig. 1, see also Ref. [7]). It is shown that the minimal value of  $J_3$  merges for both states for low amplitudes, and deviates for larger average photon numbers, starting at  $\bar{n} \approx 1$ . We note that a similar analysis was recently done for CS mixed with photon-subtracted SV [32].

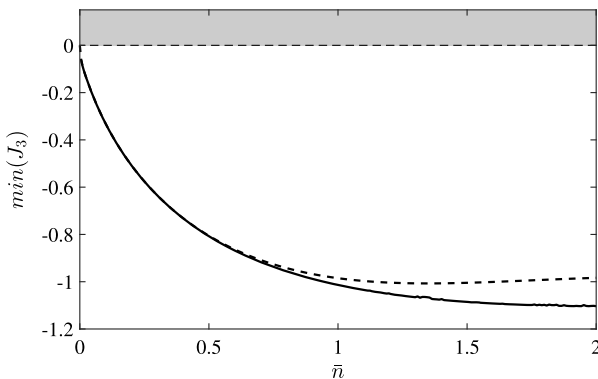


**Fig. 3.** Simulation results showing violation of the third Janssen inequality  $J_3 \leq 0$  is shown below the gray shaded area, for the state  $|\psi\rangle_{\text{out}}$  produced by mixing CS and SV with the optimal parameters of Eq. (9) (solid line), and for an ideal ECS (dashed line), as a function of the total average photon number  $\bar{n}$ .

### 3. EXPERIMENTAL SETUP AND RESULTS

Since an ECS is a superposition of NOON states for every photon number, we will show that the photon number distribution forms a corner distribution, i.e.,  $P_{N_c, N_d} = |C_{N_c, N_d}|^2$  [Eq. (7)] is approximately  $P_{N_c, N_d} = 0$  for  $N_c \neq 0$  and  $N_d \neq 0$ . The experimental setup (Fig. 4) is similar to the one used for the generation of NOON states [23,24,33]. SV is produced via spontaneous parametric down-conversion (SPDC) and is mixed with a CS with indistinguishable spatial and spectral modes. These two sources are prepared in two orthogonal polarization modes ( $H$  and  $V$ ) and are combined by a polarizing BS (PBS). A polarization-maintaining fiber with axes oriented at  $\pm 45^\circ$  ( $D, A$ ) is used to implement the BS in Fig. 1(b) in a collinear geometry. A second PBS sends the photons in each polarization mode to two photon-number resolving detectors based each on an 1:8 fiber splitter and eight single-photon avalanche photon detectors, to record  $N_c$  and  $N_d$ .

The results of the measured  $P_{N_c, N_d}$  are presented in Fig. 5. It is clear from these measurements that for any number of photons coming out of the beam, photons are highly bunched, i.e., most are going to either port  $c$  or port  $d$ . As shown in Fig. 5(b), the probability for a photon correlation, normalized for every number of measured photons (see caption, Fig. 5), is higher on the corner of the plot. An ideal ECS should have vanishing probability for all intermediate photon distributions.

In order to quantify the similarity of the multi-photon correlation measurements  $P_{m,n}$  between the approximate states and perfect ECS, we calculated  $\tilde{F} = \left( \sum_{m,n} \sqrt{P_{m,n} \cdot P_{m,n}^{\text{ECS}}} \right)^2$  [34], where  $P_{m,n}^{\text{ECS}}$  is the photon number correlation for ECS. Figure 6 presents the similarity  $\tilde{F}$  obtained by varying the amount of SV in the experimental measurements (circles) or simulation (solid line). Here,  $P_{m,n}^{\text{ECS}}$  was calculated from a simulation for perfect generation of an ECS [Eq. (1)] as would be detected in our

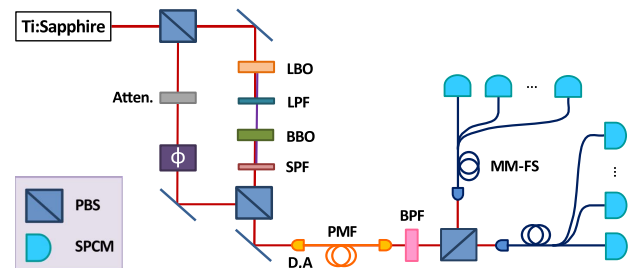


**Fig. 4.** Experimental setup for generation of entangled coherent states, detailed layout of the setup. 120-fs pulses from a Ti:sapphire oscillator operated at 80 MHz are up-converted using a lithium triborate (LBO) crystal, short-pass filtered, and then down-converted using a beta barium borate (BBO) crystal, generating a squeezed vacuum state, having correlated photon pairs at the original wavelength (808 nm). This squeezed vacuum ( $H$  polarization) is mixed with attenuated coherent light ( $V$  polarization) on a polarizing beam splitter (PBS). A thermally induced drift in the relative phase is corrected every few minutes with the use of a liquid crystal phase retarder,  $\phi$ . The spatial and spectral modes are matched using a polarization-maintaining fiber (PMF) and a 3-nm (full width at half max) bandpass filter (BPF). CS and SV are mixed by a 50/50 beam splitter transformation [Fig. 1(b)] in a collinear, polarization-based inherently phase-stable design, by using a PMF fiber aligned at  $\pm 45^\circ$  ( $D, A$ ) polarization axes, where ECSs are realized. Photon-number resolving detection is performed using an array of 16 single-photon counting modules (SPCM, Perkin Elmer), and 1:8 multi-mode fiber splitters (MM-FSs).

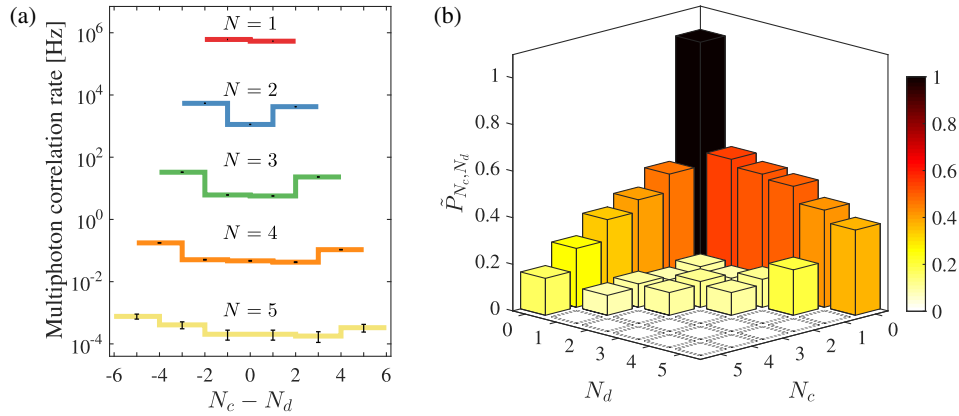


**Fig. 5.** Experimental Fock projection measurements of coherent and squeezed vacuum light interfered on a 50/50 beam splitter. (a)  $N$ -photon correlation rates plotted against the photon number difference between the output ports of the beam splitter,  $N_c - N_d$ . Error bars represent the statistical standard error of the 24 h long measurement. (b) Multiphoton correlation probabilities, normalized for every number of measured photons,  $\tilde{P}_{N_c, N_d} = P_{N_c, N_d} / (\sum_{k=0}^N P_{k, N-k})$ .

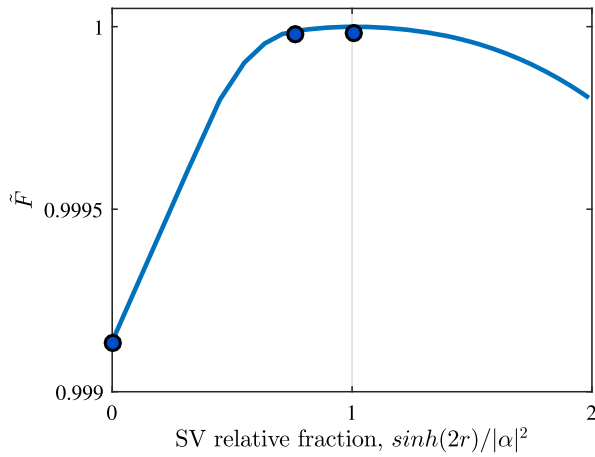


**Fig. 6.** Similarity  $\tilde{F}$  between the state generated by mixing of SV with CS and ECS in our setup, accounting for loss ( $\eta = 0.1$ , see text), for various amounts of SV, using experimental (circles) and simulated (solid line) photon correlation measurements. The approximate ECS is achieved for the optimal SV fraction of  $\sinh(2r)/|\alpha|^2 = 1$  [Eq. (9)], showing maximal similarity to ECS.

setup, accounting for our detection scheme and losses ( $\eta = 0.1$ ), using no fit parameters [23,24]. The CS amplitude was decreased from  $\beta = 0.75$  to  $\beta = 0.45$ , as the fraction of SV increased. These results show that a maximal similarity is achieved for its optimal parameters of Eq. (9). We note that the experimental state has non-zero off-corner terms, as can be seen in Fig. 5. These terms reduce the similarity to an ECS, but their contribution is exponentially small due to their exponentially small probabilities compared with the probabilities on the corner.

#### 4. DISCUSSION

The measurements presented in Fig. 5 could have appeared to result from a mixed state. To show that this is not the case, and rather that these states are in fact ECS, we have derived a measure for the purity of ECS in our scheme. Our measurements

suggest that states in our setup are indeed close to pure ECS (see Supplement 1).

Our method provides a simple and deterministic route to generate ECSs. We achieve amplitude values that are comparable with previous experimental realizations, while these relied on a photon-subtraction technique, resulting in an indeterministic photon source [14]. ECSs have also been realized recently in super-conducting circuits deterministically [35]; however, translating these states to traveling waves, as typically required in application of quantum metrology and quantum communications, has not been demonstrated yet.

The average photon number of the state in our experimental realization was  $\bar{n} = 0.15$ , for which the fidelity to ECS is theoretically  $F \approx 1$  (see Fig. 2). Previous measurements of quantum state tomography in  $N$ -photon subspaces of the states generated in our setup have shown high fidelities to NOON states [24], in agreement with ECS [Eq. (1)]. Scaling up our approach to higher average photon numbers is therefore highly desired, where high-fidelity ECS with  $\bar{n} \sim 1$  should be achievable, using a more energetic source of SV (e.g., Ref. [13]). It should be noted that even low amplitude could prove to be beneficial in some applications, e.g., it was recently shown that there is an advantage in using low-amplitude ECS ( $|\alpha| \approx 1$ ) over larger ones for quantum communication [36].

Imperfections in the experiment had two main causes. One reason involved the distinguishability between two independent photons from the CS and SV state, which limits their interference visibility (two-photon interference visibility is  $v = 0.91 \pm 0.02$  with 95% confidence level; see Supplement 1) and mainly increases the probability for  $P_{N_c, N_d}$  for  $N_c, N_d \neq 0$ . The other reason has to do with the fiber splitters. Coupling efficiency difference of about 12.8% as well as non-uniform splitting ratios result in skewness of the plots in Fig. 5, toward port  $d$ .

Furthermore, while in the ideal case of photon number detection, the state is simply projected on the photon number basis [Eq. (7)], in the experiment, detection scheme and loss could affect the measurement. In these cases, higher photon numbers in the state are also partially projected to lower photon numbers in the measurement outcome in either mode,  $c$  or  $d$  [see Fig. 1(b)]. Using a simulation of our system accounting for these inefficiencies, the theoretical photon number distribution of the generated

state can be found, with no fit parameters [23]. Interestingly, these inefficiencies preserve the photon number corner distributions, since photon loss events reduce probabilities from higher photon numbers along either side of the corner to lower photon numbers along that same side of the corner.

It is interesting to note that (bright) displaced squeezing uses a setup similar to the one described in Fig. 1(b), but with much stronger intensities. These experiments are typically performed with the objective of achieving quantum noise reduction [26]. Our work shows that extending the concept of CS and SV interference to the weak amplitude regime can be particularly useful in generating maximally entangled states, such as ECSs.

## 5. SUMMARY

In summary, we have shown that the interference of coherent light and squeezed light on a BS can generate low-amplitude ECS with high fidelity. These states violate a Bell-type inequality, similar to ECSs. We have experimentally realized these states and analyzed them through photon number detection, showing a pronounced corner-like two-mode distribution of photons, with maximal overlap for an optimal fraction of SV and coherent light. Our method benefits from a relatively simple setup that allows a deterministic route to generating ECSs without resorting to inefficient photon subtraction. Such an approach could become useful for long-distance entanglement distribution [37], particularly with low amplitudes [36] and using lossy channels [38].

**Funding.** DIP–German-Israeli Project Cooperation; BSF-NSF (2014719); Icore–Israeli Centre of Research Excellence (“Circle of Light”); Crown Photonics Center.

See Supplement 1 for supporting content.

## REFERENCES

1. A. Aspect, P. Grangier, and G. Roger, “Experimental realization of Einstein-Podolsky-Rosen-Bohm Gedanken experiment: a new violation of Bell’s inequalities,” *Phys. Rev. Lett.* **49**, 91–94 (1982).
2. M. M. Weston, M. J. W. Hall, M. S. Palsson, H. M. Wiseman, and G. J. Pryde, “Experimental test of universal complementarity relations,” *Phys. Rev. Lett.* **110**, 220402 (2013).
3. P. Shadbolt, J. C. F. Mathews, A. Laing, and J. L. O’Brien, “Testing foundations of quantum mechanics with photons,” *Nat. Phys.* **10**, 278–286 (2014).
4. V. Giovannetti, S. Lloyd, and L. Maccone, “Advances in quantum metrology,” *Nat. Photonics* **5**, 222–229 (2011).
5. I. A. Walmsley, “Quantum optics: science and technology in a new light,” *Science* **348**, 525–530 (2015).
6. B. C. Sanders, “Entangled coherent states,” *Phys. Rev. A* **45**, 6811–6815 (1992).
7. C. C. Gerry, J. Mimih, and A. Benmoussa, “Maximally entangled coherent states and strong violations of Bell-type inequalities,” *Phys. Rev. A* **80**, 022111 (2009).
8. B. C. Sanders, “Review of entangled coherent states,” *J. Phys. A* **45**, 244002 (2012).
9. K. Park and H. Jeong, “Entangled coherent states versus entangled photon pairs for practical quantum-information processing,” *Phys. Rev. A* **82**, 062325 (2010).
10. J. Joo, W. J. Munro, and T. P. Spiller, “Quantum metrology with entangled coherent states,” *Phys. Rev. Lett.* **107**, 083601 (2011).
11. A. Luis, “Equivalence between macroscopic quantum superpositions and maximally entangled states: application to phase-shift detection,” *Phys. Rev. A* **64**, 054102 (2001).
12. H. Takahashi, K. Wakui, S. Suzuki, M. Takeoka, K. Hayasaka, A. Furusawa, and M. Sasaki, “Generation of large-amplitude coherent-state superposition via ancilla-assisted photon subtraction,” *Phys. Rev. Lett.* **101**, 233605 (2008).
13. T. Gerrits, S. Glancy, T. S. Clement, B. Calkins, A. E. Lita, A. J. Miller, A. L. Migdall, S. W. Nam, R. P. Mirin, and E. Knill, “Generation of optical coherent-state superpositions by number-resolved photon subtraction from the squeezed vacuum,” *Phys. Rev. A* **82**, 031802 (2010).
14. A. Ourjoumtsev, F. Ferreyrol, R. Tualle-Brouri, and P. Grangier, “Preparation of non-local superpositions of quasi-classical light states,” *Nat. Phys.* **5**, 189–192 (2009).
15. C. C. Gerry, “Generation of optical macroscopic quantum superposition states via state reduction with a Mach-Zehnder interferometer containing a Kerr medium,” *Phys. Rev. A* **59**, 4095–4098 (1999).
16. C. C. Gerry, A. Benmoussa, and R. A. Campos, “Nonlinear interferometer as a resource for maximally entangled photonic states: application to interferometry,” *Phys. Rev. A* **66**, 013804 (2002).
17. M. Paternostro, M. S. Kim, and B. S. Ham, “Generation of entangled coherent states via cross-phase-modulation in a double electromagnetically induced transparency regime,” *Phys. Rev. A* **67**, 023811 (2003).
18. S. Glancy and H. M. de Vasconcelos, “Methods for producing optical coherent state superpositions,” *J. Opt. Soc. Am. B* **25**, 712–733 (2008).
19. J. Dowling, “Quantum optical metrology—the lowdown on high-NOON states,” *Contemp. Phys.* **49**, 125–143 (2008).
20. Y. M. Zhang, X. W. Li, W. Yang, and G. R. Jin, “Quantum Fisher information of entangled coherent states in the presence of photon loss,” *Phys. Rev. A* **88**, 043832 (2013).
21. H. F. Hofmann and T. Ono, “High-photon-number path entanglement in the interference of spontaneously down-converted photon pairs with coherent laser light,” *Phys. Rev. A* **76**, 031806 (2007).
22. L. Pezzé and A. Smerzi, “Mach-Zehnder interferometry at the Heisenberg limit with coherent and squeezed-vacuum light,” *Phys. Rev. Lett.* **100**, 073601 (2008).
23. I. Afek, O. Ambar, and Y. Silberberg, “High-NOON states by mixing quantum and classical light,” *Science* **328**, 879–881 (2010).
24. Y. Israel, I. Afek, S. Rosen, O. Ambar, and Y. Silberberg, “Experimental tomography of NOON states with large photon numbers,” *Phys. Rev. A* **85**, 022115 (2012).
25. L. A. Rozema, J. D. Bateman, D. H. Mahler, R. Okamoto, A. Feizpour, A. Hayat, and A. M. Steinberg, “Scalable spatial superresolution using entangled photons,” *Phys. Rev. Lett.* **112**, 232602 (2014).
26. C. C. Gerry and P. L. Knight, *Introductory Quantum Optics* (Cambridge University, 2005).
27. J. Joo, K. Park, H. Jeong, W. J. Munro, K. Nemoto, and T. P. Spiller, “The enhanced phase estimation using quantum Fisher information in nonclassical continuous-variable states and its application,” in *Proceedings of the First International Workshop on ECS and Its Application to QIS* (2013).
28. C. C. Gerry, A. Benmoussa, and K. M. Bruno, “Single-mode squeezed vacuum states as approximate Schrödinger phase cats: relation to  $su(1, 1)$  phase operators,” *J. Opt. B* **5**, 109–115 (2003).
29. R. Jozsa, “Fidelity for mixed quantum states,” *J. Mod. Opt.* **41**, 2315–2323 (1994).
30. S. Janssens, B. D. Baets, and H. D. Meyer, “Bell-type inequalities for quasi-copulas,” *Fuzzy Sets and Systems* **148**, 263–278 (2004).
31. C. F. Wildfeuer, A. P. Lund, and J. P. Dowling, “Strong violations of Bell-type inequalities for path-entangled number states,” *Phys. Rev. A* **76**, 052101 (2007).
32. F. Töppel, M. V. Chekhova, and G. Leuchs, “Conditionally generating a mesoscopic superposition of NOON states,” arXiv:1607.01296 (2016).
33. Y. Israel, S. Rosen, and Y. Silberberg, “Supersensitive polarization microscopy using NOON states of light,” *Phys. Rev. Lett.* **112**, 103604 (2014).
34. A. Peruzzo, M. Lobino, J. C. Matthews, N. Matsuda, A. Politi, K. Poulios, X.-Q. Zhou, Y. Lahini, N. Ismail, K. Wörhoff, Y. Bromberg, Y. Silberberg, M. G. Thompson, and J. L. O’Brien, “Quantum walks of correlated photons,” *Science* **329**, 1500–1503 (2010).
35. C. Wang, Y. Y. Gao, P. Reinhold, R. Heeres, N. Ofek, K. Chou, C. Axline, M. Reagor, J. Blumoff, K. Sliwa, L. Frunzio, S. M. Girvin, L. Jiang, M. Mirrahimi, M. H. Devoret, and R. J. Schoelkopf, “A Schrödinger cat living in two boxes,” *Science* **352**, 1087–1091 (2016).
36. N. Sangouard, C. Simon, N. Gisin, J. Laurat, R. Tualle-Brouri, and P. Grangier, “Quantum repeaters with entangled coherent states,” *J. Opt. Soc. Am. B* **27**, A137–A145 (2010).
37. J. B. Brask, I. Rigas, E. S. Polzik, U. L. Andersen, and A. S. Sørensen, “Hybrid long-distance entanglement distribution protocol,” *Phys. Rev. Lett.* **105**, 160501 (2010).
38. Y. Lim, J. Joo, T. P. Spiller, and H. Jeong, “Loss-resilient photonic entanglement swapping using optical hybrid states,” *Phys. Rev. A* **94**, 062337 (2016).